

Experimental Analysis of DC Water Pumps with Non-Geared and Geared Mechanism in Air Cooler Prototypes

M. Syahmi Aiman¹, K. Anuar Mohamad^{1*}

¹ Department of Electrical Engineering, Faculty of Electrical and Electronic Engineering, Universiti Tun Hussein Onn Malaysia, 86400, Batu Pahat, Johor, MALAYSIA

*Corresponding Author: khairulam@uthm.edu.my

DOI: <https://doi.org/10.30880/eeee.2025.06.02.034>

Article Info

Received: 27 June 2025

Accepted: 08 July 2025

Available online: 30 October 2025

Keywords

DC water pumps, geared and non-geared mechanism, prototypes of air coolers, energy efficiency, ESP32 microcontroller, real-time monitoring

Abstract

The paper includes the results of the conducted experiment on DC water pumps performance, which have geared and non-geared mechanisms built into prototypes of air coolers. The research is intended to analyze electrical and thermal performance such as power usage, the stability of current, temperature condition, and efficiency at a specific test condition. A monitoring system was developed with the ESP32 microcontroller using real-time data sensors and uploaded in Google sheets through Wi-Fi. Experimental results showed that non-geared pumps achieved an average efficiency between 80–85% with lower current usage (0.36–0.38 A) and more stable temperature (21.81–26.50 °C), while geared pumps showed lower efficiency (70–75%) and higher current draw (0.41–0.46 A). This suggests non-geared pumps are more suitable for energy-limited or tropical locations in sustainable air-cooling systems.

1. Introduction

The warm weather of Malaysia requires appropriate cooling systems which are energy-efficient and less costly. Although air conditioners provide necessary cooling, they consume a lot of power, thus they lack viability in energy-limited regions [1]. Evaporative-based air coolers, however, are becoming popular due to the bounties it affords in energy consumption and green appeal [2]. Direct current (DC) water pumps in such systems are very essential in pumping water around the cooling medium. The pumps are normally categorized into; non-geared (direct drive) and geared pumps all with their own distinct properties. The non-geared pumps have simpler construction, less moving parts, less noise and are simpler to maintain whereas the geared pumps consist of gear mechanisms which are used to govern the flow and the pressure but adds more mechanics [3], [4]. The paper examines the thermal and electric efficiency of the two types of pumps in aid of the creation of cost-effective and sustainable air cooler systems [5], [6].

DC-powered air coolers are more energy-efficient than conventional air conditioning systems as they consume less power and are suitable for open or semi-enclosed spaces in tropical climates such as Malaysia [7]. However, most commercially available air coolers use general-purpose DC water pumps, which have not been thoroughly evaluated for long-term durability, voltage stability, current consistency, and cooling efficiency. The two main categories of such pumps—geared and non-geared—differ significantly in structure and performance, where geared pumps offer steady pressure and flow, while non-geared pumps are simpler, quieter, and more energy-efficient [8][9]. Despite these distinctions, there is a lack of focused experimental studies comparing both pump types under identical operating conditions [10].

Therefore, this project evaluates and compares the electrical and thermal performance of geared and non-geared DC water pumps within the same air cooler system. It aims to establish their appropriateness for sustainable cooling in environments with limited power. A parallel test platform is created to ensure that both

precise and independent measurements in the case of both non-gearred and geared pumps. In particular, the non-gearing pump temperature, voltage, current sensors were attached to pins GPIO34, GPIO35 and GPIO36, whereas the temperature, voltage, current sensors of the geared pump were attached to the following nodes GPIO39, GPIO32 and GPIO33. Stable power to ESP32 was provided through USB connection to a laptop, and DC motors with their PWM speed controllers were driven with an outside 12V DC power supply adapter. Such division of sources of power provided a separation of signals, minimized electrical noise, and the stability of sensor reading. The sensor wiring diagram is presented in Fig. 3 by presenting the manner in which the system incorporates physical inputs to enable real-time data logging with ESP32 microcontroller.

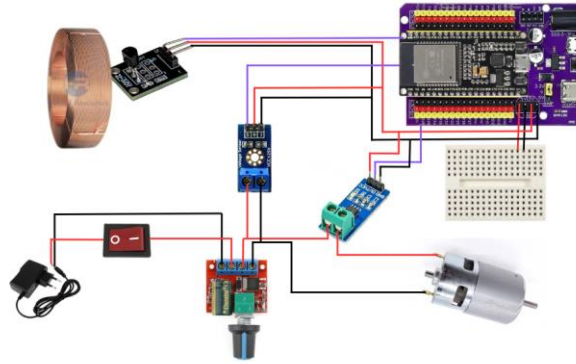


Fig. 3 Wiring Connection of the IoT-based Air Cooler System

2.3. IoT Data Logging System

2.3.1. Arduino IDE and ESP32 Programming

The Arduino IDE was used in programming the ESP32 microcontroller to control data collection of all sensors. It was developed in C++ and availed of the basic libraries, including WiFi.h, HTTPClient.h, OneWire.h, and DallasTemperature.h as shown in Fig. 4. The use of these libraries allowed Wi-Fi communication and correct sensor connection. In the code, ESP32 measured the voltage, current, and temperature of individual pump systems. Based on the data obtained, the microcontroller calculated its output power, where $P = V \times I$ and its system efficiency as $(\text{Output Power} / \text{Input Power}) \times 100$. Whereas Fig. 5 shows the data collection was set timed every ten minutes to avoid the issue of blockings and the millis () function was utilized. The results were announced on the Serial Monitor and at the same time prepared to be uploaded on the cloud.

```

1 //===== LIBRARIES =====
2 #include <WiFi.h>
3 #include <HTTPClient.h>
4 #include "ACS712.h"
5 #include <OneWire.h>
6 #include <DallasTemperature.h>

```

Fig. 4 Library Reference

```

44 //===== Timing Variables =====
45 unsigned long previousMillis = 0;
46 const unsigned long interval = 10UL * 60UL * 1000UL; // 10 menit = 600 000 ms

```

Fig. 5 Time Delay Code

2.3.2. Google Sheets as Cloud-Based Data Logger

ESP32 was configured to send data to google sheets as GET requests. Fig. 6 shows a Google Apps Script was used to achieve a Web App Script URL, which the ESP32 can use to post values and the result comparing the two sensors. Among the data sent, there was a motor temperature, current, input and output voltage, output power, and efficiency in timestamp-ordered data. This system enabled real time viewing of the system performance to be carried out on the web without any actual contact made.

```

1 function doGet(e) {
2   Logger.log(JSON.stringify(e));
3   var result = "OK";
4
5   if (!e.parameter) {
6     return ContentService.createTextOutput("No Parameters");
7   }
8
9   var sheet_id = "1eS2ofzc88InYbcDsFqul9in5LG_EjBdpSX01ArkLoE"; // Your actual Sheet ID
10  var sheet_name = "DATA 1"; // Your sheet name
11
12  var sheet = SpreadsheetApp.openById(sheet_id).getSheetByName(sheet_name);
13
14  // Always start from row 3
15  var newRow = Math.max(3, sheet.getLastRow() + 1);
16
17  var rowData = [];
18
19  // Motor 1 Data
20  var currDate = Utilities.formatDate(new Date(), "Asia/Kuala_Lumpur", "dd/MM/yyyy");
21  var currTime = Utilities.formatDate(new Date(), "Asia/Kuala_Lumpur", "HH:mm:ss");
22  rowData[0] = currDate; // A
23  rowData[1] = currTime; // B
24  rowData[2] = Number(e.parameter.temp1 || 0); // C
25  rowData[3] = Number(e.parameter.current1 || 0); // D
26  rowData[4] = Number(e.parameter.vin1 || 0); // E
27  rowData[5] = Number(e.parameter.vout1 || 0); // F
28  rowData[6] = Number(e.parameter.power1 || 0); // G
29  rowData[7] = Number(e.parameter.eff1 || 0); // H
30
31  // Add a gap (Column I)
32  rowData[8] = ""; // I (Gap column)
    
```

Fig. 6 App Script Coding for Google Sheets Table

Fig. 7 shows data was auto coded to new rows, thus resulting in clean data format that would be further analyzed. Google Sheets provided a scalable, free, accessible environment that made remote data visualization quite easy.

| MOTOR 1 (NO GEAR) | | | | | | | | MOTOR 2 (WITH GEAR) | | | | | | | |
|-------------------|----------|-------|----------|------|-------|--------|-------|---------------------|-------|----------|------|-------|--------|-------|--|
| Date | Time | Temp1 | Current1 | Vin1 | Vout1 | Power1 | Eff1 | Time | Temp2 | Current2 | Vin2 | Vout2 | Power2 | Eff2 | |
| 13/06/2025 | 17:43:36 | 32.88 | 1620.85 | 12.3 | 9.04 | 14.66 | 73.53 | 17:43:36 | 32.94 | 1232.43 | 12.3 | 9.01 | 11.1 | 73.22 | |
| 13/06/2025 | 17:44:35 | 32.88 | 1362.83 | 12.3 | 9.03 | 12.31 | 73.41 | 17:44:35 | 32.94 | 1031.22 | 12.3 | 9 | 9.28 | 73.19 | |
| 13/06/2025 | 17:45:35 | 32.88 | 1965.33 | 12.3 | 9.04 | 17.76 | 73.48 | 17:45:35 | 32.94 | 955 | 12.3 | 9.07 | 8.66 | 73.73 | |
| 13/06/2025 | 17:46:35 | 32.88 | 1368.69 | 12.3 | 9.03 | 12.36 | 73.41 | 17:46:35 | 32.88 | 1263.98 | 12.3 | 9.09 | 11.49 | 73.92 | |

Fig. 7 Table data Google Sheets

2.3.3. Flow of IoT Communication

Based on the Fig. 8 shows the four steps of data pipeline in the whole IoT communication system. In the initial step, the sensors took analog data in the geared and non-gearred configuration of the pump. The ESP32 read and computed these raw values and computed performance metrics associated with these raw values. Next, ESP32 used Wi-Fi connection to send the information and form an HTTP GET send. Only after that, the request was sent to the Google Apps Script Web URL where the incoming data were parsed and logged in the corresponding cells of the spreadsheet. The provided communication model guaranteed that the hardware-to-cloud data transfer occurred in real-time and without any asynchrony, thus creating a whole IoT monitoring loop. Fig. 8 demonstrates the entire flow of communication used to send the information between sensors in cloud logging.

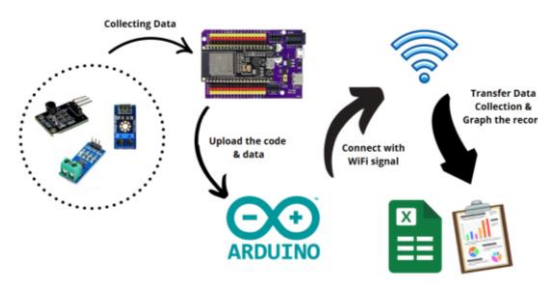


Fig. 8 Flow of Transferring Coding System

3. Results and Discussion

In this segment, the results of the tests of the performance of geared and none geared DC water pumps conducted on the basis of real-time logged data in Google sheets via an ESP32 based IoT infrastructure are shown. Voltage, current, temperature, power and efficiency electrical and thermal values were collected at regular intervals (10-minute interval) under the same conditions of test. This comparison emphasizes the ratings in performance stability, energy consumption, and temperature behavior. Analysis of each pump behavior and based on the tables and graphs, further conclusions could be drawn regarding efficiency, current draw, and thermal trends of two types of pumps.

3.1. Performance Analysis Through Google Sheets

The experiment to check the performance of geared and non-geared DC water pumps was conducted with the use of the ESP32 microcontroller that sent sensor readings to Google sheets in real-time. These data comprised input voltage, current, temperature, power, and efficiency calculation. This logging procedure was repeated once after every 10 minutes during this testing cycle resulting in detailed information comparing the two types of pumps with the same test environment and load. The tabulated findings made the motor behavior and performance changes, especially between the current draw and the thermal trends easy to observe.

The non-geared pump also consumed less current on average with an average of between 0.36A and 0.38A compared to the geared pump with more and variable current of between 0.41A and 0.46A. The increased current electricity consumption of the geared motor means that more energy is consumed because of the mechanical load added by the gears system required by the geared motor. There was an impact on thermal performance too; the non-geared pump had a steadier average operating temperature of 33.5°C, compared with a higher temperature profile in the geared pump which reached a highest 38.4°C. Internal losses are reflected in the increased amount of heat that is generated in the geared pump and may lead to efficiency of its operation and the wear over a longer period.

The logged data was also used as revealed in efficiency calculations of the non-geared pump showing that it was more efficient. It could always perform with levels of efficiency of 80 percent and 85%, whereas the geared pump had a bit lower value, which were usually recorded as 70% and 75%. Fig. 9 presents the screenshot of a part of the data which is recorded in Google Sheets with the observed values which are logged in real time. In these trends, it is implied that the non-geared pump did not only use less amount of energy, but it also worked better and with a constant manner when compared to the working conditions applied to it. Google Sheets cloud-based logger was also found to be a convenient and sufficient means of constant monitoring in that the system performance could be accessed with great ease without any physical effort to retrieve the information.

| MOTOR 1 (NO GEAR) | | | | | | | |
|-------------------|----------|------------|---------------|----------|-----------|------------|----------|
| Date | Time | Temp1 (°C) | Current1 (mA) | Vin1 (V) | Vout1 (V) | Power1 (W) | Eff1 (%) |
| 15/06/2025 | 13:31:56 | 21.81 | 1517.90 | 12.3 | 8.98 | 13.63 | 73.00 |
| 15/06/2025 | 13:41:56 | 22.00 | 1423.76 | 12.3 | 8.89 | 12.65 | 72.24 |
| 15/06/2025 | 13:51:56 | 22.25 | 1400.90 | 12.3 | 8.94 | 12.52 | 72.65 |
| 15/06/2025 | 14:01:51 | 23.06 | 1556.74 | 12.3 | 8.90 | 13.86 | 72.39 |
| 15/06/2025 | 14:11:52 | 23.87 | 1597.90 | 12.3 | 8.93 | 14.27 | 72.61 |
| 15/06/2025 | 14:21:51 | 24.50 | 1127.97 | 12.3 | 8.92 | 10.07 | 72.56 |
| 15/06/2025 | 14:31:51 | 25.19 | 1076.69 | 12.3 | 8.92 | 9.61 | 72.56 |
| 15/06/2025 | 14:41:51 | 25.56 | 1042.25 | 12.3 | 8.95 | 9.33 | 72.80 |
| 15/06/2025 | 14:51:51 | 25.00 | 1009.38 | 12.3 | 8.94 | 9.02 | 72.65 |
| 15/06/2025 | 15:01:51 | 26.50 | 1076.71 | 12.3 | 9.12 | 9.82 | 74.12 |

(a) Motor 1 (No Gear)

| MOTOR 2 (WITH GEAR) | | | | | | | |
|---------------------|----------|------------|---------------|----------|-----------|------------|----------|
| Date | Time | Temp2 (°C) | Current2 (mA) | Vin2 (V) | Vout2 (V) | Power2 (W) | Eff2 (%) |
| 15/06/2025 | 13:31:56 | 26.37 | 1099.41 | 12.3 | 9.00 | 9.89 | 73.14 |
| 15/06/2025 | 13:41:56 | 27.13 | 777.48 | 12.3 | 8.93 | 6.95 | 72.63 |
| 15/06/2025 | 13:51:56 | 27.50 | 895.51 | 12.3 | 8.94 | 8.00 | 72.65 |
| 15/06/2025 | 14:01:51 | 27.87 | 780.60 | 12.3 | 8.92 | 6.97 | 72.56 |
| 15/06/2025 | 14:11:52 | 28.12 | 1026.00 | 12.3 | 8.90 | 9.13 | 72.36 |
| 15/06/2025 | 14:21:51 | 28.12 | 929.38 | 12.3 | 8.93 | 8.30 | 72.58 |
| 15/06/2025 | 14:31:51 | 28.50 | 875.04 | 12.3 | 8.94 | 7.82 | 72.65 |
| 15/06/2025 | 14:41:51 | 29.06 | 798.00 | 12.3 | 8.91 | 7.11 | 72.46 |
| 15/06/2025 | 14:51:51 | 28.87 | 729.39 | 12.3 | 8.94 | 6.52 | 72.70 |
| 15/06/2025 | 15:01:51 | 29.06 | 588.98 | 12.3 | 9.16 | 5.39 | 74.44 |

(b) Motor 2 (With Gear)

Fig. 9 The Google Sheets Data Logging Figure

3.2. Graphical Analysis of Results

Fig. 10 shows the trend of efficiency with time of non-geared and the geared DC water pumps. The line graph of the non-geared pump was more stable, and efficiency increased steadily up to a value of 85%, as opposed to the geared pump, which decreased in efficiency during test period. Conversely, the figure illustrated that the geared pump had an irregular efficiency value in the range of 70-75%. The discrepancy of a few percentage points of the average efficiency of the order of 10% is major in the low-power systems, and it is more so when long-term runs are put into consideration or even solar-based sources. The increased efficiency of the non-geared pump indicates less loss of mechanical energy as it has a very simple direct-drive theme and hence it converts more electrical energy to useful mechanical result.

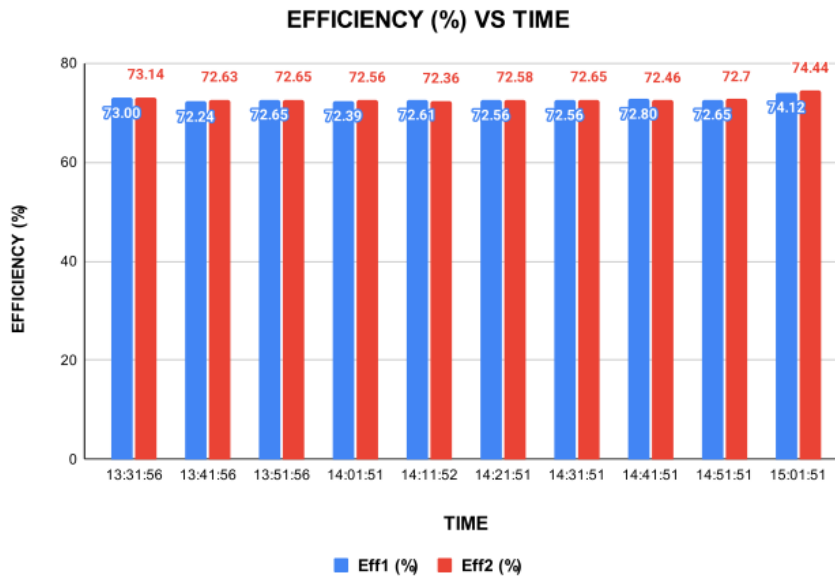


Fig. 10 Graph Chart for Efficiency vs Time

Fig. 11 demonstrates the power output (Watt) of both pumps over the period of operation. This non-gearred pump had less difference in power with 4.5 W to 5.0 W, as compared to the geared pump. The geared pump, however, recorded a broader variation between the values 5.2 W and 6.0 W. What this implies is that not only did the geared pump consume more power, it also did not maintain consistency in output and the gear mechanism may have contributed to more load resistance. The increased need for higher power, together with reduced efficiency, implies that the geared pump consumes more power to achieve the same cooling effect and this should not be ideal in systems that have fewer power sources or where the design emphasis is more on energy savings.

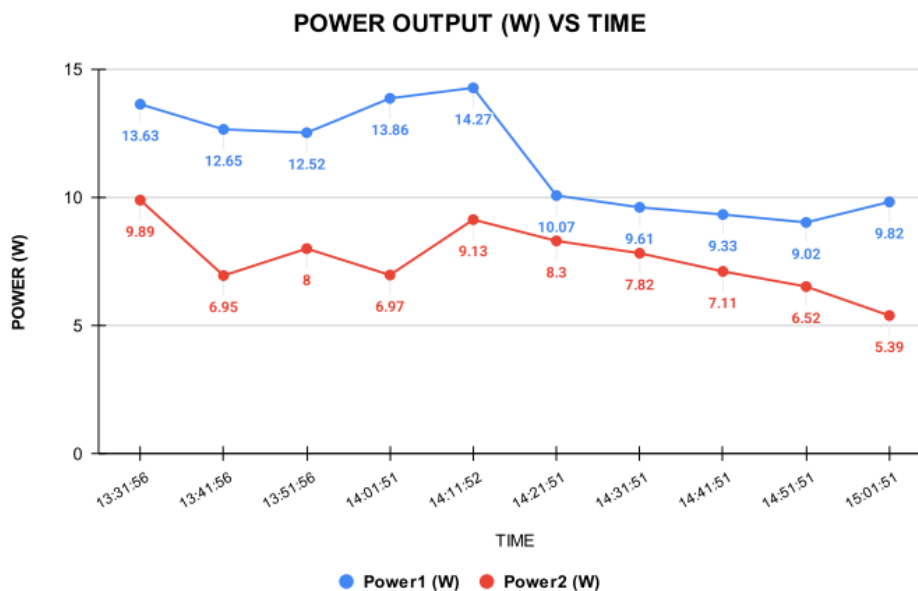


Fig. 11 Graph Chart for Power Output vs Time

The current draw (Ampere) of the two pump types is presented in Fig. 12 against time. The non-gearred pump was using less and more constant current values with typical current ranging between 0.36 A and 0.38 A. In the meantime, geared pump exhibited a more volatile current, between 0.41 A and 0.46 A. This current variation translates to load and internal resistance instability and imposes even greater burden on the power supply. In the long term, such no smooth current draw may influence the dependability of connected components, especially in systems with batteries or controlled sources like solar inverters.

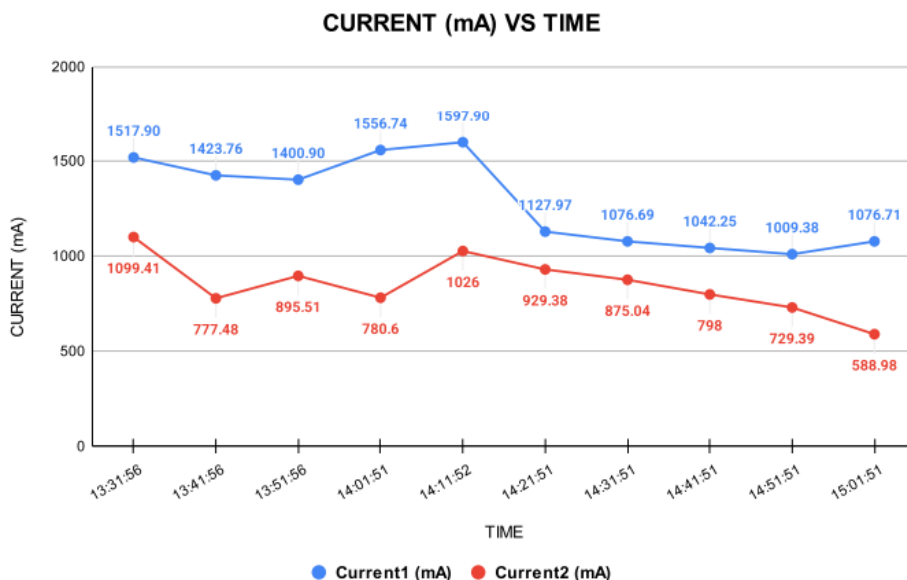


Fig. 12 Graph Chart for Current vs Time

To bring out correlation, Fig. 13 is done in a dual-line chart showing the temperature and efficiency of the two pumps. The flatter and lower temperature curve of the non-gearred motor extended through the test to an average of 33.5°C and on an equal amount of efficiency curve runs nearly 83%. However, the geared pump experienced increasing temperatures which reached the maximum of 38.4°C and the efficiency curve followed the same pattern of decline. In this comparison, it is evident as to how internal heat generation in the geared motor helps in decreased performance. Energy losses are caused by heat being produced by mechanical friction or resistance, and a decrease in the overall efficiency of any system, which further confirms the benefits of a thermally stable motor design.

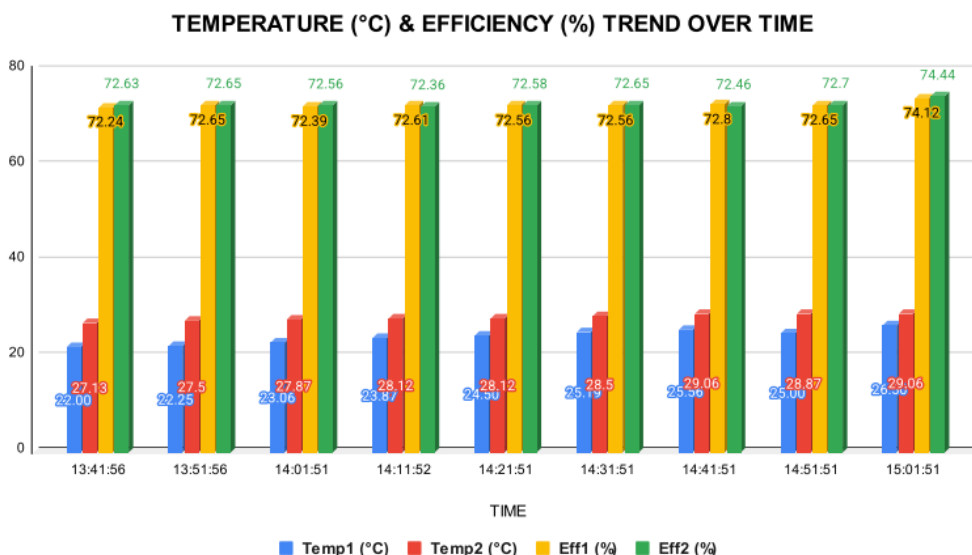


Fig. 13 Graph Chart for Temperature and Efficiency Trend Over Time

The trend of output power and efficiency was compared with time in Fig. 14. In the non-gearred pump, the two parameters had a persistent and positive tendency because as power was increasing modestly, the efficiency did not decrease but instead it was constant. Conversely, there was an unstable interconnection between the power and the efficiency of the geared pump, as there were signs of its temporary drop even when the output power was great. This can be blamed on what is lost internally through power e.g. mechanical resistance and friction, where the energy is lost to heat instead of useful translation into the flow of water. The non-gearred pump therefore shows greater use of power and balance of performance.

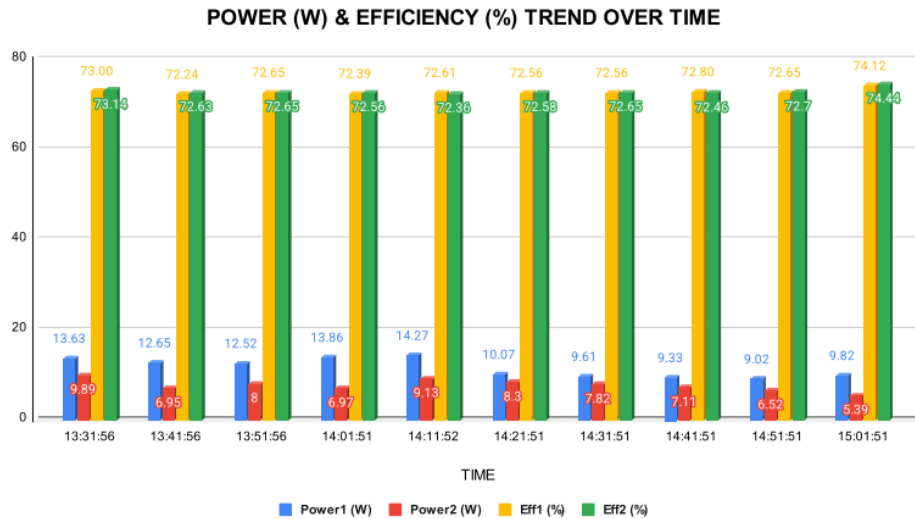


Fig. 14 Graph Chart for Power and Efficiency Trend Over Time

Fig. 15 indicates how current and temperature trends of both motors change in the course of time. The non-gear pump once more demonstrated parallel consistencies in the two parameters viz: rectangular current and level-low temperature line. In the geared motor, high temperatures were registered immediately after high currents and these observations meant that more electricity flow resulted in more heat generation, which was not efficient and could cause damage in the long run when running continuously. This direct current-to-heat relationship again confirms the fact that non-gear pumps are cooler running, more efficient and more able to stand longer in low energy systems.

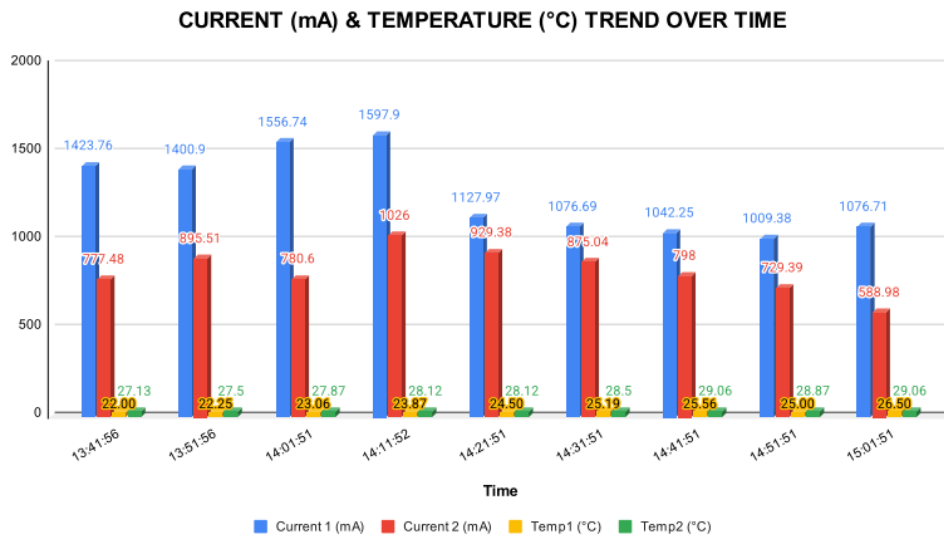


Fig. 15 Graph Chart for Current and Temperature Trend Over Time

4. Conclusion

This paper has been able to design and experiment with an air cooler prototype model based on geared and non-gear 12V DC water pumps. Pump performances in terms of electrical and thermal characteristics were measured in real time using ESP32, and cloud logging was performed with Google Sheets. It was proved experimentally that under the same conditions, the non-gear DC pump had higher energy efficiency, lower operating temperature, and more consistent current behavior than the geared pump. This indicates that the non-gear pumps are appropriate for low-cost, energy-efficient air-cooling systems, especially in energy-limited or tropical regions. Real-time monitoring and data logging were also successful in incorporating an IoT-enabled monitoring strategy, providing a scalable solution for similar implementations. Future work may focus on enhancing the durability and performance of the system by integrating pi-type thermal insulation, applying signal filtering for sensor stability, and incorporating moisture control strategies. These improvements can further optimize the cooling efficiency and long-term operation of DC-powered air cooler systems.

Acknowledgement

This work was supported by Universiti Tun Hussein Onn Malaysia (UTHM) through Multi-Disciplinary Research Grant (MDR) (vot Q772).

Conflict of Interest

Authors declare that there is no conflict of interest regarding the publication of the paper.

Author Contribution

The authors confirm contribution to the paper as follows: **study conception and design:** M. Syahmi Aiman; **data collection:** M. Syahmi Aiman; **analysis and interpretation of results:** M. Syahmi Aiman; **draft manuscript preparation:** M. Syahmi Aiman. **manuscript verification:** K. Anuar Mohamad. All authors reviewed the results and approved the final version of the manuscript

References

- [1] Zhang, P., Guo, B., & Wang, L. (2023). An experimental study on the heat and mass transfer characteristics of an evaporative cooler. *Energies*, 16(21), 7330.
- [2] Hassan, Z., & Siambun, N. J. (2020). *Experimental performance analysis of a direct evaporative cooler*.
- [3] W. Li, L. Ji, L. Ma, Y. Yang, L. Zhou, and R. K. Agarwal, "Numerical and experimental study of variable speed automobile engine cooling water pump," *Science Progress*, vol. 103, no. 2, Apr. 2020, doi: <https://doi.org/10.1177/0036850420925227>.
- [4] "Gear Pumps vs Diaphragm Pumps - Advantages and Disadvantages," *www.graco.com*. <https://www.graco.com/us/en/in-plant-manufacturing/solutions/articles/how-electric-diaphragm-pumps-can-solve-typical-issues-related-to-gear-pumps.html>
- [5] S. Abaranji, K. Panchabikesan, and V. Ramalingam, "Experimental Investigation of a Direct Evaporative Cooling System for Year-Round Thermal Management with Solar-Assisted Dryer," *International Journal of Photoenergy*, vol. 2020, pp. 1–24, Dec. 2020, doi: <https://doi.org/10.1155/2020/6698904>.
- [6] M. M. Muhsen, A. A. Abdulrasool, and B. R. Sadiq, "Experimental study on performance improvement of air cooler incorporating two-stages," vol. 1067, no. 1, pp. 012112–012112, Feb. 2021, doi: <https://doi.org/10.1088/1757-899x/1067/1/012112>.
- [7] Y. Arifin, M. Sarjan, and A. Indrajaya, "Comparison of the input photovoltaic water pump with and without floating cooling system," *MATEC Web of Conferences*, vol. 331, p. 03002, 2020, doi: <https://doi.org/10.1051/mateconf/202033103002>.
- [8] M. Yazar, "Comparative efficiency and performance analysis of spur gear and non-circular (square) gear hydraulic pumps," *Flow Measurement and Instrumentation*, vol. 102, p. 102817, Mar. 2025, doi: <https://doi.org/10.1016/j.flowmeasinst.2025.102817>.
- [9] A. Mitov, N. Nikolov, and I. Kralov, "Influence of the Radial Gap on the External Gear Pump Performance," *Applied Sciences*, vol. 15, no. 2, p. 907, 2025, doi: <https://doi.org/10.3390/app15020907>.
- [10] Z. Hassan, Mohd Suffian Misaran@Misran, and N. J. Siambun, "Experimental Performance Analysis of a Direct Evaporative Cooler," *Journal of Advanced Research Design*, vol. 67, no. 1, pp. 1–8, 2020, Accessed: Jun. 14, 2025. [Online]. Available: <https://akademiabaru.com/submit/index.php/ard/article/view/4925>
- [11] A. Ganesha, S. Kumar, N. Kumar, H. Girish, Anala Krishna Harsha, and Matam Vidya Sekhar, "Performance evaluation of an indirect-direct evaporative cooler using aluminum oxide-based nanofluid," *Journal of Thermal Analysis and Calorimetry*, vol. 148, no. 23, pp. 13543–13557, Nov. 2023, doi: <https://doi.org/10.1007/s10973-023-12652-w>.